

# Microsequential injection: anion separations using 'Lab-on-Valve' coupled with capillary electrophoresis

Chao-Hsiang Wu, Louis Scampavia and Jaromir Ruzicka\*

Department of Chemistry, Box 351700, University of Washington, Seattle, WA 98195-1700, USA

Received 28th February 2002, Accepted 16th May 2002

First published as an Advance Article on the web 10th June 2002

Microsequential injection ( $\mu$ SI) has been successfully coupled with capillary electrophoresis (CE). Presented is the  $\mu$ SI-CE system, interfaced with an integrated Lab-on-Valve (LOV) manifold that provides an efficient sample delivery conduit and a versatile means of sample pretreatment along with total automation of the separation process. Programmable  $\mu$ SI protocols control all critical system peripherals to perform various types of CE sample injections automatically such as electrokinetic (EK) injection, hydrodynamic (HD) injection, and head column field amplification (HCFA) sample stacking injection. Novel features of the  $\mu$ SI-CE technique are demonstrated on assays of samples containing 10 anions that had been used previously as a model system. Calibration studies by EK sample injection yielded linear concentration ranges of 0.5–3.0 mM with linear regression responses of  $r^2 = 0.9999$  for both chloride and sulfate using conductivity corrected peak area (CCPA) as concentration responses. Calibration using an internal standard was studied at the same concentration range giving  $r^2 = 0.9992$  for both chloride and sulfate and  $r^2 = 0.9997$  for both when CCPA correction was deployed. With HCFA sample stacking injection, a linear concentration dynamic range of 0.034–3.419 mM for chloride and 0.014–1.408 mM for sulfate were produced with linear regression responses of  $r^2 = 0.9999$  for chloride and  $r^2 = 0.9998$  for sulfate.

## Introduction

Capillary electrophoresis (CE) or high performance CE (HPCE) has been widely used in bioanalytical research. CE is now serving as a powerful tool in an ever growing scope of applications, although CE is still somewhat lagging behind well established routine applications, mainly because sample injection, sample pretreatment, and mobile phase modifications are not yet fully automated.

Karlberg, Kuban, as well as Fang *et al.* were the first to propose the method of flow injection (FI) as a front end to CE with the aim of automating the injection process. Both groups developed the idea into a full spectrum of practical applications summarized in Table 1. Their work presents an amazing variety of ingenious approaches such as the determination of metallo-cyanides by FI-liquid membrane-CE,<sup>1</sup> use of gas diffusion in measuring volatile species in soft drinks, vinegar, and wine<sup>2</sup>, detection of small anions,<sup>3,4</sup> hydrodynamic (HD) sample injection,<sup>5</sup> and on-line monitoring for kraft pulping liquors.<sup>6</sup>

Fang *et al.* developed an interface between FI and CE comprising of a horizontal sample splitting device which combined electrokinetic (EK) and hydrodynamic (HD) sample injection mechanisms<sup>7</sup> for chiral separations,<sup>8</sup> enabling sample preconcentration with use of an on-line sorption column,<sup>9</sup> and allowing the monitoring of drug dissociation.<sup>10</sup> They used conventional flow injection (FI) for sample delivery and for background electrolyte (BGE) buffer refreshment around the electrodes. Since the carrier was driven by peristaltic pump(s), it was difficult to pressurize the system and deploy HD sample injection in addition to which EK sample injection has long been recognized as having an inherent problem of sampling discriminations.<sup>11</sup>

The pioneering work of Karlberg, Kuban, and Fang clearly demonstrated the advantages of FI-CE. It has become apparent that the combination of microsequential injection ( $\mu$ SI) with capillary electrophoresis ( $\mu$ SI-CE) would be even more advantageous for the following reasons: The  $\mu$ SI system, driven by a single syringe pump, can pressurize the system with the

Table 1 FI-CE related articles

Apparatus	Applications	Detection	Ref.
FI-liquid membrane-CE	Metallo-cyanide complexes (Co(CN) <sub>6</sub> <sup>3-</sup> , Pd(CN) <sub>4</sub> <sup>2-</sup> , Fe(CN) <sub>6</sub> <sup>3-</sup> , Au(CN) <sub>2</sub> <sup>-</sup> , and Ag(CN) <sub>2</sub> <sup>-</sup> )	Direct-UV ( $\lambda = 214$ nm)	1
Gas diffusion-FI-CE	HS <sup>-</sup> , SO <sub>3</sub> <sup>2-</sup> , formate, HCO <sub>3</sub> <sup>-</sup> , acetate in soft drinks, vinegar, and wine	Indirect-UV ( $\lambda = 372$ nm)	2
Dialysis-FI-CE	Small anions in fruit pulp and milk	Indirect-UV ( $\lambda = 372$ nm)	3
FI-CE	Calibration principles of EK injection (Cl <sup>-</sup> , SO <sub>4</sub> <sup>2-</sup> , and NO <sub>3</sub> <sup>-</sup> )	Indirect-UV ( $\lambda = 372$ nm)	4
FI-CE	Evaluation of HD injection (Na <sup>+</sup> , Ca <sup>2+</sup> , Mg <sup>2+</sup> , and Li <sup>+</sup> )	Indirect-UV ( $\lambda = 262$ nm)	5
FI-CE	On-line monitoring of SO <sub>3</sub> <sup>2-</sup> , Br <sup>-</sup> , Cl <sup>-</sup> , SO <sub>4</sub> <sup>2-</sup> , NO <sub>2</sub> <sup>-</sup> , and NO <sub>3</sub> <sup>-</sup> in kraft pulping liquors	Indirect-UV ( $\lambda = 372$ nm)	6
FI-CE	Improvement of sample injection (magnolol and benzoic acid)	Direct-UV ( $\lambda = 224$ nm)	7
FI-CE	Chiral separation of intermediate enantiomers in chloramphenicol synthesis	Direct-UV ( $\lambda = 278$ nm)	8
FI-CE	On-line sorption preconcentration column for pseudoephedrine	Direct-UV ( $\lambda = 210$ nm)	9
FI-CE	Dissolution of trimethoprim (TMP) and sulfamethoxazole (SMZ)	Direct-UV ( $\lambda = 224$ nm)	10
FI-CE	Drug dissolution of ibuprofen tablets	Direct-UV ( $\lambda = 222$ nm)	33
FI-CE	Development of bias-free sample introduction method (Cl <sup>-</sup> , SO <sub>4</sub> <sup>2-</sup> , NO <sub>3</sub> <sup>-</sup> , and F <sup>-</sup> )	Indirect-UV ( $\lambda = 254$ nm)	34
SI-CE	Chip-based CE using SI for sample introduction of FITC-labeled amino acids	Laser-induced Fluorescence (LIF)	35

aim of carrying out HD injection of the sample into the capillary and of exchanging or refreshing the BGE buffer in the capillary. The  $\mu$ SI system is an excellent tool for sample dilution, preconcentration, and/or purification. It is also an excellent tool for capillary preparation, conditioning, and reactivation. While conventional FI operates at a milliliter (mL) scale,  $\mu$ SI operates at a microliter ( $\mu$ L) scale which is equally compatible with micro-FIA systems<sup>6</sup> and meets CE requirements and many research needs.

The versatility of  $\mu$ SI in a 'Lab-on-Valve' (LOV) configuration has recently been demonstrated in a number of papers listed in Table 2 where LOV has been used as a sample processing 'front end' to UV-VIS spectrometry, electrothermal atomic absorption spectrometry (ETAAS), as well as mass spectrometry (MS) in environmental, biotechnological, clinical, and trace element assays.

The separation of anions, used by Kuban and Karlberg in their FI-CE work as a model system,<sup>4</sup> is used to demonstrate the advantages of the marriage between the powerful separation mechanisms of electrophoresis with the automation concepts of the microsequential injection technique. A conventional  $\mu$ SI-LOV system (Fig. 1a, right) was interfaced with a homemade CE system (Fig. 1a, left) using the flow-through cell component of the LOV to which a CE capillary and cathode were inserted. The outflow channel was furnished with an open/close isolation valve that allowed all fluid channels to be pressurized by the syringe pump. Samples containing 10 anions were separated and detected by indirect UV detection using chromate as a BGE additive. Due to the nature of the analytes, the CE was operated under reversed polarity with an electroosmotic flow (EOF) suppressed by BGE modifier cetyltrimethylammonium bromide (CTAB).<sup>12</sup>

## Experimental

### System components

The apparatus shown in Fig. 1 was controlled by the following components. A stepper motor driven syringe pump (XL 3000, CAVRO Scientific Instruments, Inc., San Jose, California, <http://www.cavro.com>) equipped with a 500.0  $\mu$ L glass syringe. A microelectric actuator (Valco Instruments Co. Inc., Houston, TX, <http://www.valco.com>) which controlled a 6-way Chem-inert<sup>®</sup> selector valve (Model C22, Valco Instruments Co. Inc., Houston, TX) for aqueous channel selection. A monolithically structured PVC Lab-on-Valve (LOV) mounted on top of the 6-way selector valve serving as the  $\mu$ SI interface to the capillary electrophoresis (CE) system (Fig. 1b). A 2-way normally open isolation valve (Cat. 225K022, NResearch Inc., West Caldwell, NJ, <http://www.nresearch.com>) connected adjacent to the CE cathode on the Lab-on-Valve leading the way to the waste. All fluid channels used 1.588 mm OD, 0.7620 mm ID FEP Teflon

tubing (Cat. 1520, Upchurch Scientific, Oak Harbor, WA, <http://www.upchurch.com>). SI experiment protocols were executed by FIALab for Windows (Ver. 5.9.54, FIALab Instruments, Inc., Bellevue, WA) installed on a PC (Intel Pentium II, 300MHz, 64MB RAM) loaded with the Microsoft Windows 2000 operating system (Ver. 5.00.2195 SP2, Microsoft Inc., Edmond, WA, <http://www.microsoft.com>).

The capillary electrophoresis system consisted of two electrodes, a fused silica capillary, an in-house capillary detection chamber, HV power supply, and a personal computer used exclusively for CE data collection. The CE anode and cathode were made of platinum wires (Pt, 0.50 mm OD, Aldrich Chemical Co. Inc., Milwaukee, WI, <http://www.sigma-aldrich.com>), the cathode was bonded within 3.0 cm PEEK tubing (Cat. 1531B, 0.2540 mm ID, 1.588 mm OD, Upchurch Scientific, Oak Harbor, WA) and inserted into the Lab-on-Valve device. The CE capillary and platinum ground cathode were sealed into standard 1.588 mm OD PEEK tubing and inserted into the integrated Lab-on-Valve manifold (Fig. 1b). The background electrolyte (BGE) buffer solution was kept circulating through port#3 of the selector valve ensuring that no buffer depletion occurred around the cathode. The  $\mu$ SI system controlled all the fluidic operations including sample delivery, sample pretreatment, rapid exchange of the BGE buffer, and on-line capillary reconditioning in a fully automated fashion.

The bare Pt wire anode (total length 3.0 cm, 2.0 cm under buffer solution) was placed in a still BGE reservoir (~25 mL) at the anode side of the capillary. A polyimide coated fused silica capillary (total length 80.0 cm, 50  $\mu$ m ID, 150  $\mu$ m OD, coated with 13  $\mu$ m polyimide, Cat. 2000015, Polymicro Technologies LLC, Phoenix, AZ, <http://www.polymicro.com>) was used for CE separation. The capillary detection window, located 45.0 cm from the cathode end, was prepared by removing the polyimide coating using hot sulfuric acid (96.5%, J.T. Baker Chemical Co., Phillipsburg, NJ, <http://www.jtbaker.com>) followed by rinsing with DI water. The detection chamber (Fig. 1c) was made from a Teflon block (dimension: 25.40 mm  $\times$  25.40 mm  $\times$  12.70 mm) with two 1.588 mm ID channels perpendicular and crossing with one another at the center of the Teflon body. The capillary was carefully positioned and centered by two 5.0 cm long, 1.588 mm OD, and 0.1778 mm ID PEEK tubing segments (Cat. 1536, Upchurch Scientific, Oak Harbor, WA). Two fiber optic cables furnished with stainless steel tips (200  $\mu$ m OD fiber, 1.588 mm OD tip, FIALab Instruments Inc., Bellevue, WA, <http://www.flowinjection.com>) were inserted into the Teflon body facing each other for data collection. A 1.588 mm OD ball lens (Cat. A46-119, Edmund Industrial Optics, Barrington, NJ, <http://www.edmundoptics.com>) was placed between the CE capillary and the UV inlet fiber optic for higher sensitivity. A deuterium UV source (Model D-1000, Analytical Instrument Systems, Inc., Flemington, NJ, <http://www.aishome.com>) was used and detection was carried out at 372 nm using a USB-interfaced UV-VIS

**Table 2** Applications using a  $\mu$ SI-LOV manifold

Apparatus	Applications	Detection	Ref.
$\mu$ SI-LOV	Fermentation monitoring of ammonium, glycerol, glucose, and free iron	Direct-UV $\lambda = 705, 540, 340,$ and $550$ nm	18
$\mu$ SI-LOV-microcolumn	Environmental monitoring of $\text{NO}_3^-$ , $\text{NO}_2^-$ , and $\text{PO}_4^{2-}$	Direct-UV $\lambda = 540$ nm for $\text{NO}_3^-$ and $\text{NO}_2^-$ ; $\lambda = 860$ nm for $\text{PO}_4^{2-}$	19
$\mu$ SI-BI-LOV	Phosphate and bioligand interaction assays of immunoglobulin (IgG) on protein G immobilized Sepharose beads	Direct-UV, $\lambda = 712$ or $880$ nm for phosphate; fluorescence $\lambda_{\text{ex}} = 450$ $\lambda_{\text{em}} = 525$ nm for bioligand assay)	29
$\mu$ SI-LOV-microcolumn-ICP-MS	Determination of Ni and Bi in human urine samples	ICP-MS	30
FI/SI-microcolumn-ETAAS	Determination of Ni in environmental and biological samples	ETAAS	31
FI/SI-microcolumn with ion-exchange beads-ETAAS	Determination of Ni in environmental and biological samples	ETAAS	32

spectrophotometer (USB2000, Ocean Optics Inc., Dunedin, FL). CE separation was driven by a high voltage power supply (CZE1000R, Spellman Inc., Hauppauge, NY, <http://www.spellmanhv.com>) working under reverse polarity mode at a constant voltage of 16.0 kV with the anode (+) side away from the  $\mu$ SI-LOV system and controlled by the PC which also controlled the  $\mu$ SI-LOV system. The CE capillary, detection chamber, BGE reservoir, Lab-on-Valve device, and the 6-way selector valve were enclosed in an in-house Plexiglas box with a built in voltage safety lock. The syringe pump and other controlling circuits of the  $\mu$ SI system were located outside the box. CE data collection was performed using the OOIBase32 spectrometer operating software (Ver. 1.0.2.0, Ocean Optics Inc., Dunedin, FL) on a personal computer (AMD-K6, 64MB RAM) using the Microsoft Windows 2000 operating system (Ver. 5.00.2195

SP2, Microsoft Inc., Edmond, WA) and a sampling frequency of 12.2 Hz.

### Reagents and standards

**Capillary conditioning solutions.** A 0.10 M sodium hydroxide wash solution was prepared from 1.0 M sodium hydroxide standard solution (Cat. VW3222-1, VWR Scientific Products, West Chester, PA, <http://www.vwrsp.com>) using 18.0 M $\Omega$  cm DI water. The DI water used was generated by a NANOpure II water purification system (at 18.0 M $\Omega$  cm, Barnstead-Thermolyne, Dubuque, IA, <http://www.barnstead.com>). All solutions, standards, and DI water were filtered through sterile 0.2  $\mu$ m Acrodisc syringe membrane filters (Cat. 4192, Pall

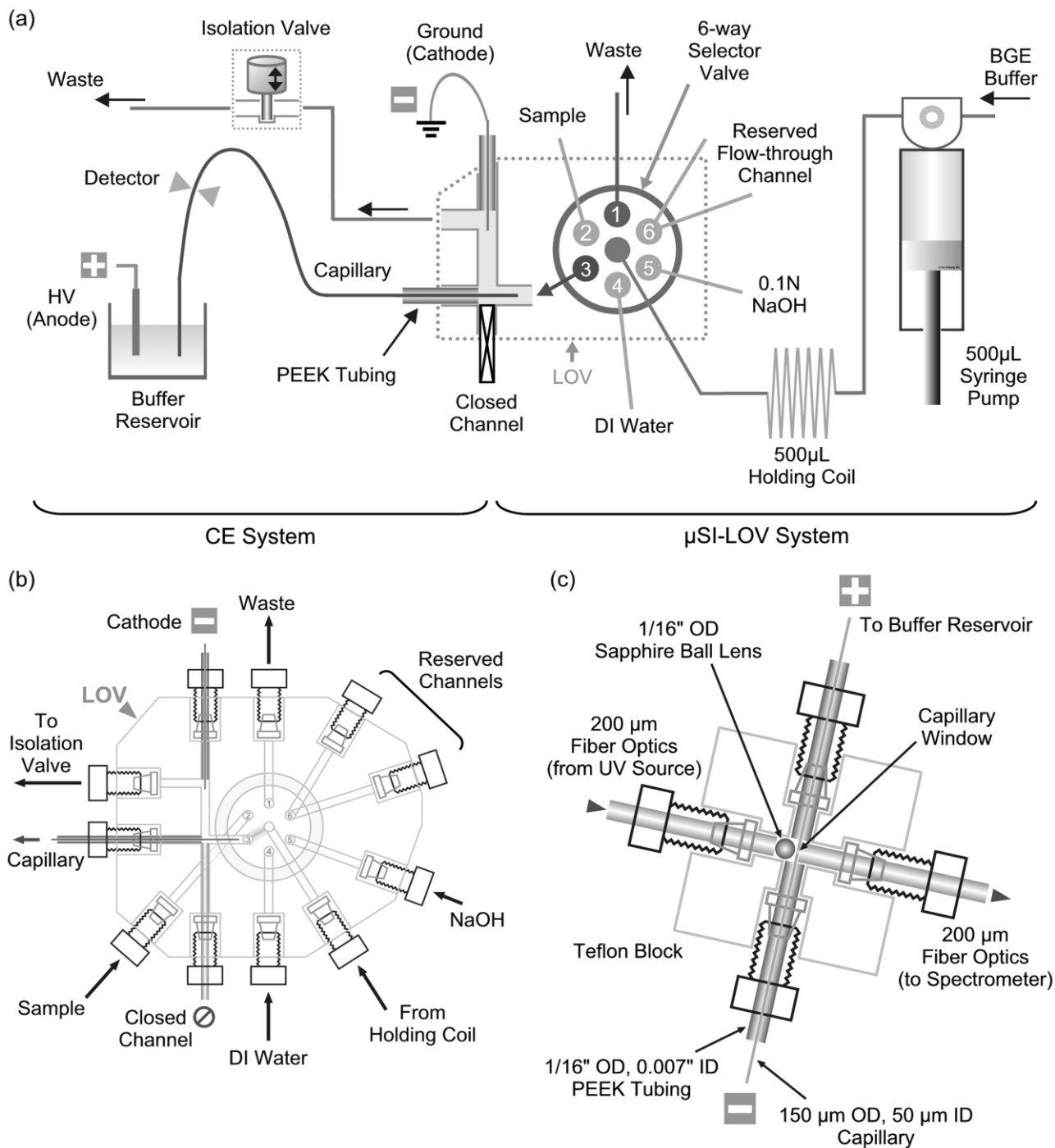


**Fig. 1** Schematic diagram of the  $\mu$ SI-CE system. (a) Using Lab-on-Valve as the interface to  $\mu$ SI and CE systems. (b) Detailed channel assignments on the Lab-on-Valve device. (c) The in-house CE detection chamber comprising of a Teflon cross made up of two 200  $\mu$ m fiber optics together with a sapphire ball lens.

Gelman Laboratory, East Hills, NY, <http://www.pall.com>) and ultrasonically degassed prior to use.

**CE background electrolyte solution.** A 0.60 M chromate stock solution was prepared by dissolving 9.718 g sodium chromate ( $\text{Na}_2\text{CrO}_4$ , Cat. 30783-1, Aldrich Chemical Co. Inc., Milwaukee, WI) in 100.0 mL DI water. A 0.10 M boric acid stock solution was prepared by dissolving 0.618 g granular boric acid ( $\text{H}_3\text{BO}_3$ , Cat. 0084-01, J.T. Baker Chemical Co., Phillipsburg, NJ) in 100.0 mL DI water. A 50.0 mM CTAB (cetrimonium bromide) stock solution was prepared by dissolving 1.822 g CTAB [ $\text{CH}_3(\text{CH}_2)_{15}\text{N}(\text{CH}_3)_3\text{Br}$ , Cat. 85582-0, Aldrich Chemical Co. Inc., Milwaukee, WI] in 100.0 mL DI water containing 5.0% (v/v) acetonitrile ( $\text{CH}_3\text{CN}$ , Cat. 11008-6, Aldrich Chemical Co. Inc., Milwaukee, WI). The final CE background electrolyte (BGE) solution was prepared by serial dilution of the stock solutions detailed above to 10.0 mM sodium chromate, 15.0 mM boric acid, and  $6.0 \times 10^{-5}$  M CTAB. The pH was adjusted with 1.0 M sodium hydroxide standard solution (Cat. VW3222-1, VWR International, West Chester, PA) to pH 7.5.

**Anion standard solution for qualitative assays.** An anion standard stock solution containing 709.4 ppm thiosulfate, 606.7 ppm chloride, 666.8 ppm nitrite, 676.4 ppm sulfate, 729.6 ppm nitrate, 733.1 ppm citrate, 452.5 ppm fluoride, 676.1 ppm phosphate, 726.3 ppm bicarbonate, and 720.8 ppm acetate was prepared by dissolving 0.157 g sodium thiosulfate 5-hydrate crystal ( $\text{Na}_2\text{S}_2\text{O}_3 \cdot 5\text{H}_2\text{O}$ , Cat. 3946-01, J.T. Baker Chemical Co., Phillipsburg, NJ), 0.100 g sodium chloride ( $\text{NaCl}$ , Cat. 3624-05, J.T. Baker Chemical Co., Phillipsburg, NJ), 0.100 g sodium nitrite ( $\text{NaNO}_2$ , Cat. 7632-00-0, Aldrich Chemical Co., Inc., Milwaukee, WI), 0.100 g sodium sulfate ( $\text{Na}_2\text{SO}_4$ , Cat. 8024, Mallinckrodt Inc., Paris, KT), 0.100 g sodium nitrate ( $\text{NaNO}_3$ , Cat. 7808, Mallinckrodt Inc., St. Louis, MO), 0.114 g sodium citrate dihydrate [ $\text{HOC}(\text{COONa})(\text{CH}_2\text{COONa})_2 \cdot 2\text{H}_2\text{O}$ , Cat. 3646-01, J.T. Baker Chemical Co., Phillipsburg, NJ), 0.100 g sodium fluoride ( $\text{NaF}$ , Cat. 7636, Mallinckrodt Inc., Paris, KT), 0.100 g sodium phosphate, dibasic anhydrous ( $\text{Na}_2\text{HPO}_4$ , Cat. 3828-01, J.T. Baker Chemical Co., Phillipsburg, NJ), 0.100 g sodium bicarbonate ( $\text{NaHCO}_3$ , Cat. 3506-01, J.T. Baker Chemical Co., Phillipsburg, NJ), and 0.166 g sodium acetate, trihydrate ( $\text{CH}_3\text{COONa} \cdot 3\text{H}_2\text{O}$ , Cat. 3460-01, J.T. Baker Chemical Co., Phillipsburg, NJ) in DI water followed by dilution to 100.0 mL. Actual working anion standard solutions were prepared by serial dilution from the standard stock solutions detailed above followed by filtration through sterile 0.2  $\mu\text{m}$  Acrodisc<sup>®</sup> syringe membrane filters (Cat. 4192, Pall Gelman Laboratory, East Hills, NY, <http://www.pall.com>). The solutions were ultrasonically degassed prior to use.

**Anion standard solutions for quantitative assays.** 100.0 mM sodium chloride/sodium sulfate standard stock solution for calibration and repeatability assays was prepared by dissolving 0.585 g sodium chloride ( $\text{NaCl}$ , Cat. 3624-05, J.T. Baker Chemical Co., Phillipsburg, NJ) and 1.420 g sodium sulfate ( $\text{Na}_2\text{SO}_4$ , Cat. 8024, Mallinckrodt Inc., Paris, KT) in 100.0 mL DI water. A 1000 mM thiosulfate standard solution for use as an internal standard was prepared by dissolving 6.205 g sodium thiosulfate 5-hydrate crystal ( $\text{Na}_2\text{S}_2\text{O}_3 \cdot 5\text{H}_2\text{O}$ , Cat. 3946-01, J.T. Baker Chemical Co., Phillipsburg, NJ) in 25.00 mL DI water. A standard stock solution containing 6066 ppm chloride and 6764 ppm sulfate for HCFA calibration was prepared by dissolving 1.000 g sodium chloride ( $\text{NaCl}$ , Cat. 3624-05, J.T. Baker Chemical Co., Phillipsburg, NJ) and 1.000 g sodium sulfate ( $\text{Na}_2\text{SO}_4$ , Cat. 8024, Mallinckrodt Inc., Paris, KT) in 100.0 mL DI water. Actual working anion standard solutions were prepared by serial dilution from the standard stock solutions detailed above followed by filtration through with sterile 0.2  $\mu\text{m}$  Acrodisc<sup>®</sup> syringe membrane filters (Cat. 4192, Pall Gelman

Laboratory, East Hills, NY, <http://www.pall.com>). The solutions were ultrasonically degassed prior to use.

## Results and discussions

### Automatic capillary initialization

A new capillary was first initialized by hydrodynamic introduction of solutions in an automated sequence of: 30.0  $\mu\text{L}$  0.10 M sodium hydroxide, 30.0  $\mu\text{L}$  DI water, and 80.0  $\mu\text{L}$  BGE buffer solution as programmed by computer control (Fig. 2). By closing the 2-way isolation valve (Fig. 1a) and positioning the 6-way selector valve at port#3 (towards the capillary), the syringe pump pressurized the whole  $\mu\text{SI-LOV}$  system forcing solution flow through the capillary. During the first period of the conditioning process, the HV power supply was automatically shut down to protect the capillary from excessive Joule heat generated by the high conductance sodium chloride wash solution. After perfusing BGE solution for 200.0 s (volume 90.0  $\mu\text{L}$ ), the conditioned BGE-filled capillary was ready for the HV power. For ensuring the best reproducibility in sample signal responses, this capillary conditioning routine was performed daily.

### Sample injection modes

Both electrokinetic (EK) and hydrodynamic (HD) sample injection modes can be carried out by using automatic  $\mu\text{SI-LOV}$  protocol software. In the EK injection mode, the injected sample segment flows through the chamber around the CE capillary while the HV is maintained at a constant potential throughout the assay cycle. In this respect, EK injection is identical to the FI-CE systems used as a model system.<sup>4</sup> In addition, HD injection can be facilitated by pressurizing the flow-through chamber by using the syringe pump with the isolation valve closed (Fig. 1a). In the HD mode, the HV power

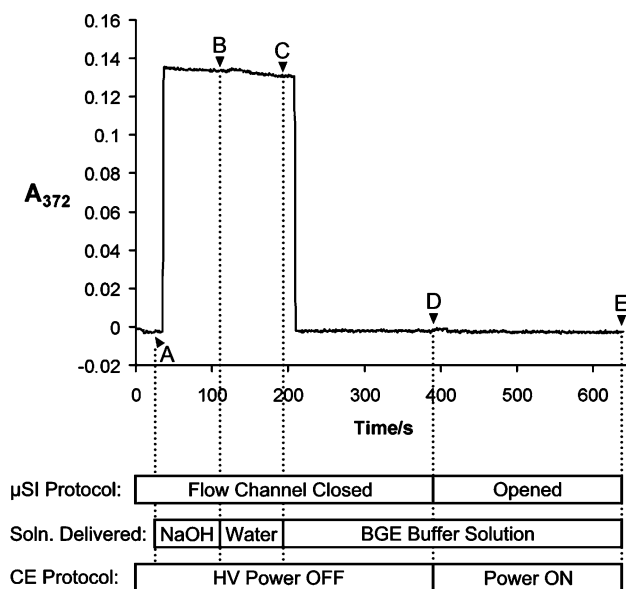


**Fig. 2** Capillary conditioning protocol. Starting with the buffer-filled capillary, the conditioning solutions, 0.10 M sodium hydroxide solution and DI water, were sequentially hydrodynamically pushed through the capillary by the combined action of the isolation valve and syringe pump. Points of interest: A: HV power was turned off, flushing the capillary with 0.1 M sodium hydroxide solution for 30.0  $\mu\text{L}$ . B: flushing with 30.0  $\mu\text{L}$  DI water. C: flushing with 80.0  $\mu\text{L}$  BGE buffer. D: HV power was turned on, isolation valve was opened, and BGE buffer was kept refreshing at the capillary injection site at flow rate of 0.5  $\mu\text{L s}^{-1}$  for 120  $\mu\text{L}$ , which extended the conditioning process as a waiting period for capillary equilibrium. E: capillary conditioning completed. The system protocol can be easily correlated with time by studying the protocol bars below.

supply was first turned off, the sample segment was then delivered at a continuous flow rate, while the isolation valve was shut for a short period and then released, so that the volume of sample injected is a function of the flow rate and the time interval that the isolation valve is closed. By combining the experimental methodologies of EK and HD injections above, a 'head column field amplification' (HCFA) sample stacking technique<sup>13</sup> was implemented.

The HCFA method is based on applying high field strength upon an injected sample zone of low conductivity. Since the conductivity of the sample is significantly lower than that of the BGE buffer, a proportionally greater electric field will develop across the sample zone causing the ions to migrate. Once the ions reach the boundary of the BGE buffer, their migration speed will become slower due to the lower electric field in the BGE buffer. This continues until all the ions in the sample zone have been concentrated into a smaller volume at the front of the sample zone allowing electrophoretic separation to begin. In the traditional CE injection process, manual manipulation of the capillary sample injection site between the sample and buffer reservoirs can cause physical disturbance of the pre-concentrated sample band leading to erroneous results. Therefore, a short plug of water (or sample solution, in this paper) was hydrodynamically injected into the capillary injection site prior to the application of the voltage. This ensures proper field amplification at the injection point. However, large amounts of injected sample can result in a deterioration of separation efficiency<sup>14</sup> and a sampling bias due to EK injection.<sup>4</sup> Therefore, the amount (or the length) of the pre-HD injected sample plug needs to be optimized. Another consideration in the use of field amplification is the generation of heat during the stacking period. Since the potential drop occurs in the sample zone, the corresponding power generation can result in a significantly elevated temperature. This can be a particular concern for thermally labile samples.<sup>15</sup> The biases in the use of EK sample injection and their correction will be discussed later.

### Indirect detection

Indirect detection is a universal detection method suitable for analytes that lack adequate light-absorbing chromophores.<sup>16</sup> The model system uses chromate to provide a UV absorbance background at 372.0 nm. The basic principle of this technique is that the analyte anions displace the chromate additive in the eluted band. Since the assay signal is provided by a displacement of chromate, a *decrease* in signal is observed for the eluted analyte band, that is, transparent sample ions create a negative absorbance peak.<sup>17</sup> Assay signals presented in this paper were all converted to positive absorbance by multiplying the results with a constant of  $-1$  for easier visual inspection (Fig. 2 to Fig. 5).

### Optimization of HCFA injection protocol

Optimal HCFA variables were obtained by injecting sample solution containing 70.94 ppm thiosulfate, 60.66 ppm chloride, and 67.64 ppm sulfate. Due to the configuration and nature of the presented  $\mu$ SI-CE system, there are three variables that need to be optimized: (1) injection point in  $\mu$ L displaced along a traditional FI profile, (2) closure time of the isolation valve under a constant flow rate, and (3) electrokinetic sample preconcentration/stacking time. When a sample segment travels along at a steady-flow, a typical FI response curve is observed due to the physical process of dispersion. By choosing the injection position using a stopped-flow technique,<sup>18,19</sup> one can control the concentration of sample by selecting the degree of dispersion between the sample and the carrier solutions. In the initial experiment (Fig. 3a), a 50.0  $\mu$ L sample was aspirated and

delivered into the capillary injection site by SI flow reversal of the syringe pump. The sample profile was then pushed forward (from 5.0  $\mu$ L to 30.0  $\mu$ L, in 5.0  $\mu$ L increments) past the capillary introduction end at a flow rate of 10.0  $\mu$ L  $s^{-1}$ . When a desired injection position was reached, the flow rate was reduced to 0.45  $\mu$ L  $s^{-1}$  and the isolation valve was then closed for an initial 5.0 s interval. Immediately after the HD injection of the sample plug into the capillary, the HV was turned on for 3.0 s (excluding a voltage ramp of 2.5 s) at 16.0 kV. Followed by the

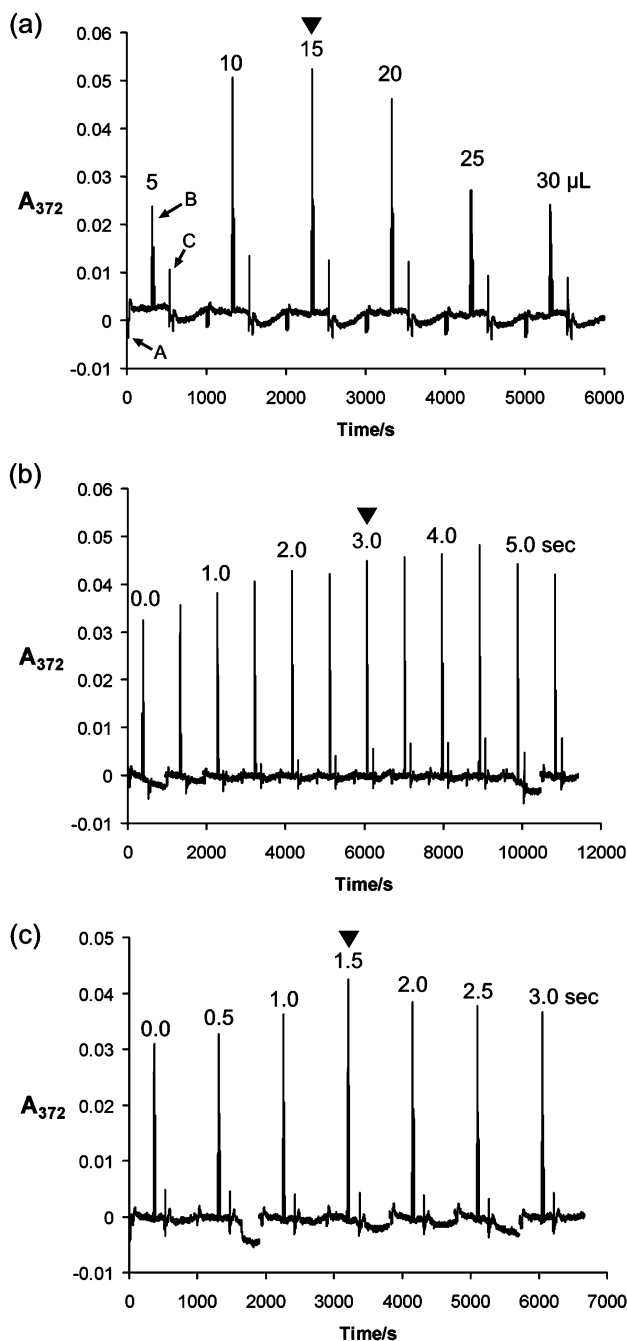


**Fig. 3** HCFA variable optimizations. Variables needed to be optimized for HCFA injection: (a) Injection point of the solution profile. Aspirated 50  $\mu$ L sample solutions were pushed from valve downstream to the capillary injection by the volumes indicated. Points of interest: A. Sample was hydrodynamically injected, electrokinetically preconcentrated, and was ready for electrophoretic separation in 10 s. B. Separated thiosulfate, chloride, and sulfate sample peaks. C. Water peak (and other ions in the capillary, if any) was hydrodynamically flushed out of the capillary by pushing BGE buffer through the capillary for returning to post-injection state. (b) Optimization for HD injection sample quantity into the capillary. (c) Optimization for the time needed for EK sample stacking. *Note:* This optimization was done without using the ball lens in the detection chamber.

introduction of fresh BGE buffer to the capillary injection site, the HV power was reactivated and electrophoresis began. During the course of electrophoretic separation, the BGE buffer was constantly refreshed at a flow rate of  $0.45 \mu\text{L s}^{-1}$  through port#3 of the selector valve with the isolation valve opened. Pushing the sample zone  $15.0 \mu\text{L}$  downstream from the selector valve, the strongest signal response was observed. This position was found to be ideal for trace enrichment when the sample amount was  $50.0 \mu\text{L}$  at a delivery flow rate of  $10.0 \mu\text{L s}^{-1}$ . Other positions can be selected if the sample concentration is too high. After separation, the capillary was flushed by closing the isolation valve with the HV power off, at a flow rate of  $0.45 \mu\text{L s}^{-1}$  in  $\mu\text{SI}$  protocol (apparent average flow rate in the capillary:  $113.0 \text{ nL s}^{-1}$ ) for 48.0 s. Note that the shape of the disposal zone in SI mode is similar to that of the FI mode for the same model system whilst operating at the microliter scale.<sup>20</sup>

By carrying over the optimized injection position of  $15.0 \mu\text{L}$ , the closure time for the isolation valve was then optimized (Fig. 3b). Note that the closure time is proportional to the sample amount that is physically injected into the capillary. It was found that having the system inject sample at a flow rate of  $0.45 \mu\text{L s}^{-1}$  for 4.5 s produces the maximum signal response. However, after close examination of the separation efficiency for each run (12 runs total), we found that the run with a 3.0 s closure time at a flow rate of  $0.45 \mu\text{L s}^{-1}$  gave the best results

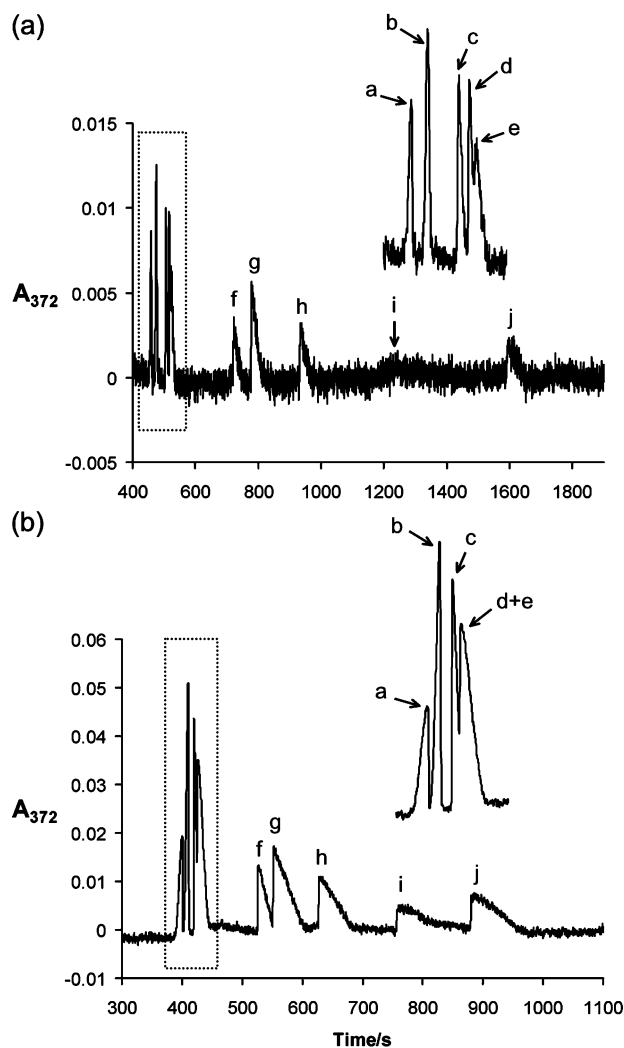


**Fig. 4** Electrochromatograms for separation of 10 anions by EK and HCFA injections. (a) Separation of 10 anions using the EK injection. a: 709.4 ppb thiosulfate, b: 606.6 ppb chloride, c: 666.8 ppb nitrite, d: 676.4 ppb sulfate, e: 729.6 ppb nitrate, f: 733.1 ppb citrate, g: 452.5 ppb fluoride, h: 676.1 ppb phosphate, i: 726.3 ppb bicarbonate, and j: 720.8 ppb acetate ions. (b) Same sample was amplified by using HCFA injection. Sulfate and nitrite were merged into one peak (d + e).

in terms of peak area, peak resolution, and reproducibility. A closure time of greater than 3.0 s resulted in a larger quantity of sample injected which resulted in poorer efficiency.<sup>14</sup> In addition, excess amount of sample in the capillary can cause current instability resulting in poor reproducibility in terms of migration time<sup>21</sup> and peak variance.<sup>22</sup> It is noticeable that the actual sample volume that has been injected can be calculated from the actual flow rate in the capillary by timing the change in absorbance during the capillary conditioning process (Fig. 2). It was calculated that the observed capillary flow rate in the capillary was  $113.0 \text{ nL s}^{-1}$ . During the optimized 3.0 s isolation valve closure interval, we thus injected a  $339.0 \text{ nL}$  sample into the capillary which is equivalent to a plug of  $172.8 \text{ mm}$  long inside the capillary ( $50.0 \text{ micron ID}$ ,  $1.962 \text{ nL mm}^{-1}$ ). It was

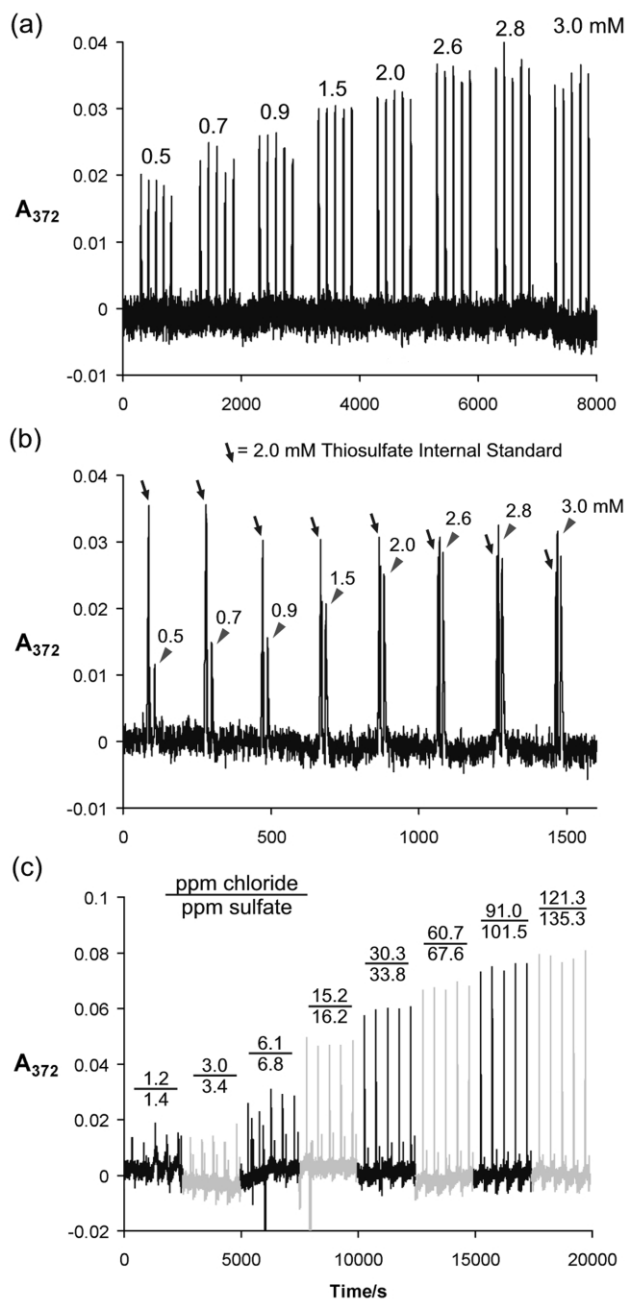


**Fig. 5** EK, IS, and HCFA calibration electrochromatograms. (a) Standards containing chloride and sulfate were injected electrokinetically (EK). Each standard solution was injected five times. (b) 2.0 mM sodium thiosulfate internal standard (IS) was added to each of the standard solutions used in (a). Each standard solution contained a fixed concentration of internal standard and was also injected five times (not shown in the figure). (c) Standard solutions containing chloride and sulfate were analyzed using the head column field amplification (HCFA) injection technique. Note: HCFA calibration was done without using the ball lens in the detection chamber.

about 21.6 % of the total capillary length (800.0 mm) and is ideal for field amplification applications.

The same methodologies were used for the optimization of the electrokinetic sample preconcentration/stacking time (Fig. 3c). The best signal responses were obtained when a total sample stacking time of 4.0 s had elapsed (= 1.5 s + 2.5 s; voltage ramping, 0.0 to 16.0 kV). A sample stacking time of less than 4.0 s resulted in an under-amplified signal; however, a stacking time of greater than 4 s resulted in the sample overheating, thus causing excess diffusion and a decrease in efficiency. Therefore, the final optimized HCFA variables were as follows: sample plug length was approximately 21.6% of the total length of the capillary with a 3.0 s isolation valve closure time and a total time for electrokinetic sample preconcentration/stacking of 4.0 s at 16.0 kV. Sample concentrations were limited to 3.5 mM maximum. No significant decreases in separation efficiency and sample temperature elevation were observed in the qualitative and quantitative assays using these optimized variables.

### Separations of 10 anions by EK and HCFA injections

A dilute sample solution containing 10 anions: 709.4 ppb thiosulfate, 606.6 ppb chloride, 666.8 ppb nitrite, 676.4 ppb sulfate, 729.6 ppb nitrate, 733.1 ppb citrate, 452.5 ppb fluoride, 676.1 ppb phosphate, 726.3 ppb bicarbonate, and 720.8 ppb acetate was used. The sample was injected by normal EK injection (Fig. 4a) and HCFA injection (Fig. 4b). For EK injection, all 10 anions were resolved and peak distortions of the last five anions were due to the mismatched mobility of the anions.<sup>23,24</sup> Enrichment factors for HCFA injection and LODs for each anion using EK and HCFA injections are listed in Table 3.

### Calibration principles

Peak area, rather than peak height, was chosen for quantitative analysis throughout the paper. Note that as sample concentration increases, electromigration dispersion begins to affect the peak shape and hence the peak width and peak height.<sup>24</sup> However, if an adequate resolution for detection can be maintained, the peak area is conserved. In addition, different degrees of sample stacking due to variance in sample ionic strength (or conductivity) can also result in loss of linearity in

**Table 3** Enrichment factors and LODs for each anion under EK and HCFA injections

Anions <sup>a</sup> (sample concentration)	LODs <sup>b</sup>		Enrichment factors <sup>c</sup> from EK to HCFA
	Using EK	Using HCFA	
a. Thiosulfate (709.4 ppb)	93 ppb	44 ppb	3.9
b. Chloride (606.6 ppb)	54 ppb	14 ppb	4.2
c. Nitrite (666.8 ppb)	74 ppb	18 ppb	3.9
d. Sulfate (676.4 ppb)	77 ppb	— <sup>d</sup>	—
e. Nitrate (729.6 ppb)	124 ppb	—	—
f. Citrate (733.1 ppb)	230 ppb	66 ppb	3.7
g. Fluoride (452.5 ppb)	89 ppb	32 ppb	4.3
h. Phosphate (676.1 ppb)	234 ppb	73 ppb	6.7
i. Bicarbonate (726.3 ppb)	521 ppb	167 ppb	8.5
j. Acetate (720.8 ppb)	345 ppb	117 ppb	5.6

<sup>a</sup> Sample containing 10 anions was injected using EK and HCFA injection methods as referred to in Fig. 4. <sup>b</sup> Values were calculated based on the peak heights of each anion in both EK and HCFA separations. Standard deviation values of blank sample in EK injection: 0.000372 (absorbance unit); in HCFA injection: 0.000392 (absorbance unit). <sup>c</sup> The factors were obtained by dividing the raw peak area from HCFA injection with the raw peak area from EK injection for each anion. <sup>d</sup> Values are not available, since sulfate and nitrate peaks in Fig. 4b were not resolved in the case of HCFA injection.

terms of peak width and peak height dependence on concentration. In this case, the peak area is still conserved.

Due to the discriminating nature of EK injections, there are two major biases that need to be compensated for before using assay data for quantitative purposes: (1) effective mobility differences of ion species and (2) bulk sample conductivity.<sup>4</sup> The amount of a particular ion species being injected is influenced by its effective mobility  $\mu_{\text{eff}}$ . If an ion has a high  $\mu_{\text{eff}}$ , then it will be overly represented at injection time. This effect causes a distortion in the ratio of peak areas for ions having different mobilities. A certain degree of correction can be made through a bias factor<sup>25</sup> based on the respective migration time for a two-species system. Moreover, Moolen *et al.* suggested that the bias caused by different effective mobility in injection and the bias in detection<sup>26</sup> are inversely proportional to each other; therefore, no correction is needed if peak areas are used for quantitative responses.<sup>27</sup> In order to evaluate this injection bias, a thiosulfate internal standard was used during calibrations. The bulk conductivity of the overall sample medium affects both electrophoretic and electroosmotic flows, ultimately changing the sample amount injected. Leube *et al.* introduced matrix-corrected peak area (COPA) using the degree of dissociation, ionic strength, and effective charge for correction of peak areas.<sup>28</sup> In this paper, we use the conductivity corrected peak area ( $A_{\text{CCPA}}$ ) method, which conveniently uses the individual peak area ( $A_i$ ) divided by a correction factor ( $f$ ). This correction factor is generated by dividing the total peak area by the bulk sample conductivities ( $\lambda_{\text{bulk}}$ ) as the quantitative responses for calibrations:

$$A_{\text{CCPA}} = \frac{A_i}{f} \quad \text{where} \quad f = \frac{\sum A_i}{\lambda_{\text{bulk}}}$$

The system performance in terms of concentration dynamic range, linearity, and repeatability using EK and/or an internal standard (Fig. 5a and b), and the HCFA injection methods (Fig. 5c) are listed in Table 4 and Table 5.

### Conclusions

The proposed  $\mu$ SI-CE system provides versatile sample pretreatments, quick capillary washout, electrolyte exchange, and automated injection by electric field and/or by pressure. Moreover, the sample can be pretreated or reacted in the LOV device prior to CE injection using classical FI or SI methodology. Different post-separation reagent based assays can also be performed using the same instrumentation since variances in experimental protocols (*e.g.* reagent addition, dilution, mixing, delivery, and incubation time) are simply programmable. The speed of performance of specific assays can be optimized if analytes of interest appear at an early stage in the electrochromatogram allowing fresh BGE buffer in the capillary to be hydrodynamically pressurized into the fluid channel to reinitialize the column faster. Capillary on-line reconditioning can be deployed as desired with no physical movement of the capillary for the best reproducible performance in this  $\mu$ SI-CE system. Sampling error can be eliminated by using the LOV device as a fixed interface to  $\mu$ SI and CE in the system presented. Since this  $\mu$ SI-CE system is configured with no physical movement of the capillary while sampling, sampling errors resulting from the disruption of the buffer boundary at the injection end can be greatly diminished. Other sources of sampling error such as excess sample evaporation, sample droplets falling out due to the movement of the robotic arm, and cross contamination resulting from sample adsorption at the outer surface of the capillary are not present in this system. The proposed  $\mu$ SI-CE system has been validated. Future work will involve more

**Table 4** Calibrations using EK injection

Conc./mM	Sodium chloride			Sodium sulfate		
	EK <sup>a</sup> /PA <sup>b</sup> (RSD%, n = 5)	EK/IS <sup>c</sup> (RSD%, n = 5)	EK/CCPA <sup>d</sup> (RSD%, n = 5)	EK/PA (RSD%, n = 5)	EK/IS (RSD%, n = 5)	EK/CCPA (RSD%, n = 5)
0.5	14.27	7.42	0.42	6.89	6.56	3.50
0.7	6.92	13.54	4.88	8.46	4.96	2.21
0.9	11.86	6.69	1.35	7.12	6.80	2.44
1.5	2.53	4.01	3.36	4.35	4.88	1.96
2.0	10.42	4.40	6.43	2.48	7.48	3.03
2.6	1.61	1.30	3.69	3.72	3.40	1.60
2.8	5.16	5.63	2.98	3.47	10.40	1.49
3.0	4.98	5.19	3.46	3.41	2.85	1.75
r <sup>2</sup>	0.9067	0.9992	0.9999	0.9297	0.9992	0.9999

<sup>a</sup> Samples were injected electrokinetically (EK). <sup>b</sup> Calibration data were calculated using raw peak areas (PA) versus ion concentrations. <sup>c</sup> Calibration data were calculated using peak area ratios of analyte areas over internal standard (IS) areas versus ion concentrations. <sup>d</sup> Calibration data were calculated using conductivity corrected peak area (CCPA) in which the conductivities of samples were measured individually. Calculated CCPA values were determined versus ion concentrations.

**Table 5** Calibrations using HCFA injection

Concentration/ mM (ppm Cl <sup>-</sup> )	Sodium chloride		Concentration/mM (ppm SO <sub>4</sub> <sup>2-</sup> )	Sodium sulfate	
	HCFA <sup>a</sup> /PA <sup>b</sup> (RSD% n = 5)	HCFA/CCPA <sup>c</sup> (RSD% n = 5)		HCFA/PA (RSD% n = 5)	HCFA/CCPA (RSD% n = 5)
0.034 (1.2ppm)	4.63	2.83	0.014 (1.4ppm)	15.32	2.93
0.085 (3.0ppm)	15.68	2.55	0.035 (3.4ppm)	17.41	2.86
0.171 (6.1ppm)	4.56	2.84	0.070 (6.8ppm)	3.91	2.04
0.427 (15.2ppm)	1.94	0.66	0.176 (16.2ppm)	2.52	0.78
0.855 (30.3ppm)	0.80	1.67	0.352 (33.8ppm)	4.30	1.99
1.709 (60.7ppm)	2.23	1.07	0.704 (67.6ppm)	3.94	1.29
2.564 (91.0ppm)	1.65	0.68	1.056 (101.5ppm)	3.04	0.83
3.419 (121.3ppm)	3.62	0.73	1.408 (135.3ppm)	3.90	0.90
r <sup>2</sup>	0.9741 <sup>d</sup>	0.9999	r <sup>2</sup>	0.9802 <sup>d</sup>	0.9998

<sup>a</sup> Samples were injected using head column field amplification (HCFA). See text for more information. <sup>b</sup> See note 'b' in Table 4. <sup>c</sup> See note 'd' in Table 4. <sup>d</sup> The regression constants were obtained using logarithmic trend lines.

advanced approaches such as capillary dynamic coating agents and novel isoelectric focusing.

## Acknowledgements

The authors would like to express their gratitude to Professor Norman J. Dovichi for the CE power supply. This research was financially supported in part by the Center for Process Analytical Chemistry (CPAC) of University of Washington and the National Institute of Health (NIH) research grant NIGMS RO1 GM45260-11 from the National Institute of General Medical Sciences.

## References

- P. Kuban, W. Buchberger and P. R. Haddad, *J. Chromatogr., A*, 1997, **770**, 329–336.
- P. Kuban and B. Karlberg, *Talanta*, 1998, **45**, 477–484.
- P. Kuban and B. Karlberg, *Anal. Chem.*, 1997, **69**, 1169–1173.
- P. Kuban, K. Tennberg, R. Tryzell and B. Karlberg, *J. Chromatogr., A*, 1998, **808**, 219–227.
- P. Kuban, R. Pirmohammadi and B. Karlberg, *Anal. Chim. Acta.*, 1999, **378**, 55–62.
- P. Kuban and B. Karlberg, *Anal. Chim. Acta.*, 2000, **404**, 19–28.
- Z.-L. Fang, Z.-S. Liu and Q. Shen, *Anal. Chim. Acta.*, 1997, **346**, 135–143.
- Z.-S. Liu and Z.-L. Fang, *Anal. Chim. Acta.*, 1997, **353**, 199–205.
- H.-W. Chen and Z.-L. Fang, *Anal. Chim. Acta.*, 1997, **355**, 135–143.
- H.-W. Chen and Z.-L. Fang, *Anal. Chim. Acta.*, 1998, **376**, 209–220.
- J. W. Jorgenson and K. D. Lukacs, *Anal. Chem.*, 1981, **53**, 1298–1302.
- K. Li and S. F. Y. Li, *J. Liq. Chromatogr.*, 1994, **17(18)**, 3889–3910.
- R.-L. Chien and D. S. Burgi, *J. Chromatogr.*, 1991, **559**, 141–152.
- M. Zhu, D. L. Hansen, S. Burd and F. Gannon, *J. Chromatogr.*, 1989, **480**, 311–319.
- A. Vinther and H. Soeberg, *J. Chromatogr.*, 1991, **559**, 27–42.
- E. S. Yeung, *Acc. Chem. Res.*, 1989, **22**, 125–130.
- E. S. Yeung and W. G. Kuhr, *Anal. Chem.*, 1991, **63(5)**, 275A–282A.
- C.-H. Wu, L. Scampavia and J. Ruzicka, *Analyst*, 2001, **126**, 291–297.
- C.-H. Wu and J. Ruzicka, *Analyst*, 2001, **126**, 1947–1952.
- P. Kuban, A. Engstrom, J. C. Olsson, G. Thorsen, R. Tryzell and B. Karlberg, *Anal. Chim. Acta.*, 1997, **337**, 117–124.
- Y. Kurosu, Y. Satou, Y. Shisa and T. Iwata, *J. Chromatogr., A*, 1998, **802**, 391–394.
- D. S. Burgi and R.-L. Chien, *Anal. Chem.*, 1991, **63**, 2042–2047.
- R. Weinberger, *Practical Capillary Electrophoresis*, 2nd. edn., Academic Press, 2000.
- R. Weinberger and M. Albin, *J. Liq. Chromatogr.*, 1991, **14(5)**, 953–972.
- X. Huang, M. J. Gordon and R. N. Zare, *Anal. Chem.*, 1988, **60**, 375–377.
- S. Hjertén, K. Elenbring, F. Kilár, J. C. Chen, C. J. Siebert and M.-D. Zhu, *J. Chromatogr.*, 1987, **403**, 47–61.
- J. N. Moolen, H. F. M. Boelens, H. Poppe and H. C. Smit, *J. Chromatogr., A*, 1996, **744**, 103–113.
- J. Leube and O. Roedel, *Anal. Chem.*, 1994, **66**, 1090–1096.
- J. Ruzicka, *Analyst*, 2000, **125**, 1053–1060.
- J. Wang and E. H. Hansen, *J. Anal. At. Spectrom.*, 2001, **16**, 1349–1355.
- J. Wang and E. H. Hansen, *Anal. Chim. Acta.*, 2000, **424**, 223–232.
- J. Wang and E. H. Hansen, *Anal. Chim. Acta.*, 2001, **435**, 331–342.
- X.-Z. Liu and Z.-L. Fang, *Anal. Chim. Acta.*, 1998, **358**, 103–110.
- Q.-S. Pu and Z.-L. Fang, *Anal. Chim. Acta.*, 1999, **398**, 65–74.
- Q. Fung, F.-R. Wang, S.-L. Wang, S.-S. Liu, S.-K. Xu and Z.-L. Fang, *Anal. Chim. Acta.*, 1999, **390**, 27–37.